

The Braess's Paradox in Dynamic Traffic

Dingyi Zhuang^{1*}, Yuzhu Huang^{1*}, Vindula Jayawardana²³, Jinhua Zhao¹, Dajiang Suo²⁴, Cathy Wu¹²

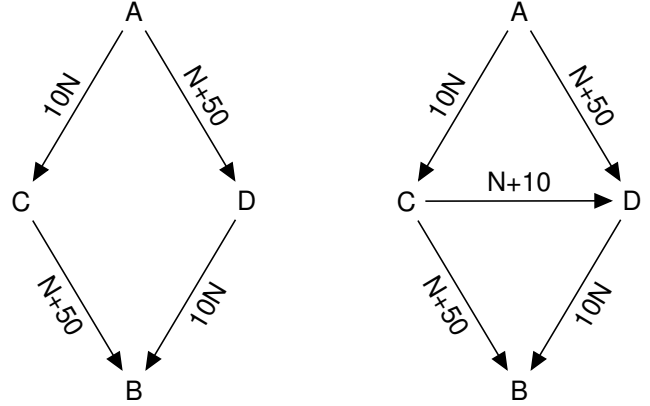
Abstract—The Braess's Paradox (BP) is the observation that adding one or more roads to the existing road network will counter-intuitively increase traffic congestion and slow down the overall traffic flow. Previously, the existence of the BP is modeled using the static traffic assignment model, which solves for the user equilibrium subject to network flow conservation to find the equilibrium state and distributes all vehicles instantaneously. Such approach neglects the dynamic nature of real-world traffic, including vehicle behaviors and the interaction between vehicles and the infrastructure. As such, this article proposes a *dynamic* traffic network model and empirically validates the existence of the BP under dynamic traffic. In particular, we use microsimulation environment to study the impacts of an added path on a grid network. We explore how the network flow, vehicle travel time, and network capacity respond, as well as when the BP will occur.

I. INTRODUCTION

A. Background

Dietrich Braess, a German mathematician, discovered that adding a new road to an existing road network, although increasing capacity, could actually exacerbate overall congestion. He argued that if each vehicle is making self-interested routing decisions, the shortest path would be frequently selected, which will lead to impedance on a shortcut and slow down overall traffic speed in the end [1], [2]. A classical approach to formulating this problem usually involves using road cost function related to the number of vehicles on each road to solve for the traffic equilibrium equations and demonstrate the BP [3].

To see how to solve the equilibrium for the BP, consider a classical static traffic assignment example. As shown in Fig. 1a, the four-edge diamond-shaped network, suppose there are six cars that wish to travel from point A to point B via routes ACB or ADB . The travel cost (usually means travel time) associated with each road segment is marked beside the edge, where N is the number of vehicles in the same road segment. Intuitively, that means that if there are more vehicles in the same road, traffic tends to congest and travel time is consequently larger. Since the cost function of each route is the same for routes ACB and ADB (if CD is not connected), the demand is evenly distributed because using one route is just as good as using the other. The user



(a) The basic four-edge network

(b) The five-edge network

Fig. 1: The classical Braess's Paradox example with static traffic assignment, where N represents the number of vehicles on the edge. If vehicles reach equilibrium, adding a path (i.e. connection CD in b) will make the traffic worse.

equilibrium reaches when three cars use route ACB and the other three choose ADB with travel cost $C_{ACB} = 30 + 53 = 83 = C_{ADB}$. Now, suppose a new shortcut CD connecting the two routes is constructed, as shown in Fig. 1b. The four-edge network is reformed to the five-edge one. Vehicles will shift to the shortcut until a new user equilibrium is reached when $C_{ACDB} = C_{ACB} = C_{ADB}$, when two vehicles are assigned to each route and the travel cost is 92 for each route, larger than the previous case without the shortcut. From this example, we could see that adding a new road to the network could in fact increase the travel time for everybody, which is the Braess's Paradox.

B. Motivation

The application of static traffic assignment on the four-edge and five-edge networks is widely discussed in previous literature on Braess's Paradox [?], [4], [5]. These works analyze the BP from the network science perspective. For the convenience of optimization, the vehicle behaviors and the routing strategy are usually simplified. Vehicles are homogeneous and their route choices are assigned instantaneously after solving the flow conservation and user equilibrium. Wolf et al. [6] proposed the TASEP framework to study the BP, but only discuss the random and fixed routing of vehicles. The lack of consideration of vehicle behaviors makes the results less empirical in real-world scenario. Colombo, Rinaldo M., Helge Holden, and Francesca Marcellini modeled the BP

*Dingyi Zhuang and Yuzhu Huang have contributed equally.

¹ Department of Civil and Environmental Engineering, Massachusetts Institute of Technology dingyi@mit.edu; yuzhuh@mit.edu; jinhua@mit.edu

² Laboratory for Information and Decision Systems, Massachusetts Institute of Technology vindula@mit.edu; cathywu@mit.edu

³ Department of Electrical Engineering and Computer Science, Massachusetts Institute of Technology

⁴ Department of Mechanical Engineering, Massachusetts Institute of Technology djsuo@mit.edu

from the microscopic vehicular traffic, but still requires a lot of constraints and assumptions to solve the Nash equilibrium [7]. Recently, Belov, Aleksandr, et al. [8] studied the price of anarchy from the Braess network using the microsimulation. The price of anarchy is the index between the user equilibrium and the system optimal. They have also discussed the network parameters and their impacts on the price of anarchy and related it with the BP. To be differentiated, our work has designed a estimated travel time based routing strategy and discuss directly the added path's impact on the network and the BP.

Moreover, under a static traffic assignment model, another crucial hidden assumption is that vehicles are assigned instantaneously. This assumption is impractical as in the real world, vehicle behaviors are dynamically changing with the surrounding environment rather than instantaneously determined. Moreover, the junction effects and the interactions of human drivers are not fully studied. Therefore, we wish to examine whether BP exists in dynamic setting. Our approach is to mimic the vehicle behaviors and analyze the network performance from the microscopic perspective. In this paper, we use the Flow project and SUMO [9], [10] as the microsimulation environment to design minimalistic scenarios and explore the characteristics of BP in the dynamic setting. Our main contributions include two parts:

- We extend the static traffic assignment problem formulation into the microsimulation context to model the BP
- Under dynamic traffic, we empirically explore the impacts of an added path on the network flow, network capacity, and vehicle travel time, and confirm the existence of BP in dynamic traffic

To our best knowledge, we are the first to analyze the BP from the dynamic microsimulation setting.

II. A DYNAMIC BRAESS'S PARADOX MODEL

A. Preliminaries

Fig. 1 example shows the idea of static traffic assignment model. We briefly review its formulation and relevant extension in the dynamic traffic assignment context, before extending it to a dynamic microsimulation context [?], [5]. It assumes that the traffic network contains a set \mathcal{S} of origin-destination pairs with $n_{\mathcal{S}}$ elements, the edge set \mathcal{L} and the path route set \mathcal{P} [?], [5]. Shown in Fig. 1 example, each route $p \in \mathcal{P}$ has cost function C_p , whose mathematical formulation of the user equilibrium is given as [11]–[14]:

$$\begin{aligned} C_p(x_p^*(t)) &= \lambda_s(t), \text{ if } x_p^*(t) > 0 \\ C_p(x_p^*(t)) &\geq \lambda_s(t), \text{ if } x_p^*(t) = 0 \end{aligned} \quad (1)$$

where $C_p(\cdot)$ defines the user (travel) cost on path p , $\lambda_s(t)$ is the minimal path costs at time t , and $x_p^*(t)$ is the path flow assignment that fulfills flow conservation. In static assignment, C_p is fixed while in dynamic assignment, $C_p(t)$ varies at different time. To help keep the notation consistency when it is extended to the dynamic traffic assignment, we keep all

the variable dependent on time. The flow conservation is in the form as:

$$f_e(t) = \sum_{p \in \mathcal{P}} x_p(t) \delta_{ep}, \quad (2)$$

where $f_e(t)$ is the flow of the edge e at time t , $x_p(t)$ is the flow on route p , and δ_{ep} is a binary indicator for whether edge e is included in route p . The traffic demand $d_s(t)$ at time t must also follow flow conservation constraints:

$$\sum_{p \in \mathcal{P}} x_p(t) = d_s(t), \quad \forall s \in \mathcal{S}, \forall t. \quad (3)$$

Similarly, denote the user cost on the edge e as $C_e(\cdot)$. The user costs on paths are defined as:

$$C_p(t) = \sum_{e \in \mathcal{L}} C_e(t) \delta_{ep}, \quad \forall p \in \mathcal{P}, \forall t. \quad (4)$$

Dynamic traffic assignment takes as $C_p(t), C_e(t), d_s(t)$ as inputs and distributes vehicles by computing the flow conservation, minimizing each user's (travel) costs $\sum_{p \in \mathcal{P}} C_p(t)$, and ensuring user travel costs reach equilibrium at every time step. As shown in the Fig. 1 example, $\sum_{p \in \mathcal{P}} C_p$ is also used to show the existence of Braess's Paradox in the static setting. The design of C_p is tricky and usually simplified to depend on only the flow on the edge. Solving the user equilibrium takes longer when the traffic network size is large or when simplifying assumptions are relaxed. We try to replace it with dynamic microsimulation, where we can capture the microscopic vehicle behaviors and understand how equilibrium and the BP naturally form.

B. Problem Formulation

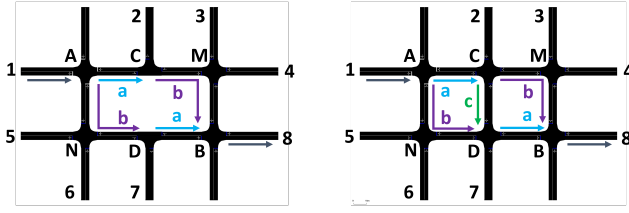
In order to mimic the real-world driving behaviors, we take a microsimulation perspective. We wish to replace the flow conservation and user equilibrium optimization with the designed routing strategy for each vehicle. Denote the driver set $\mathcal{U} = \{d_s(t)\}$ that contains the demand at time t . When choosing the route, we consider each vehicle $u \in \mathcal{U}$ has potential travel cost function C_u correlated to designed function $g(\cdot)$ of route flow, travel time, edge information:

$$C_u(t) = g(x_p(t), e, p), \quad \forall e \in \mathcal{L}, \forall p \in \mathcal{P}. \quad (5)$$

We formulate the microscopic traffic assignment model by equalizing $\sum_{u \in \mathcal{U}} C_u$ instead of $\sum_{p \in \mathcal{P}} C_p$ by solving user equilibrium, and consider the existence of the BP under this more realistic model. The introduction of C_u provides us with the microscopic leverage to discuss the important factors that will influence the vehicle routing decisions, as well as the potential impacts on the whole network.

C. Network Design

The classical diamond-shaped networks in Fig. 1 have some distinct characteristics. Traffic enters the network from node A, and leaves at node B. Before a new path is added, each route from node A to node B (A→C→B, or A→D→B, shown in Fig. 1a) has the same overall cost function; after the new path is added, the third route (A→C→D→B, shown



(a) Grid network with 2 routes (the baseline network/scenario). (b) Grid network with an added path (the add-path network/scenario).

Fig. 2: A 2-by-3 grid network resembling the classical diamond network.

in Fig. 1b) has a different cost function that makes it more preferable than the original routes.

To model this classical network under the microsimulation setting, we designed a grid network that resembles the diamond network, as shown in Fig. 2. There are a total of 6 intersections, all are controlled with all-way stops except for intersection A. Arrows denote the directions of traffic flow. In the basic design, shown in Fig. 2a, two routes are available, namely $A \rightarrow C \rightarrow M \rightarrow B$ and $A \rightarrow N \rightarrow D \rightarrow B$. With an additional path added, as shown in Fig. 2b, a third route $A \rightarrow C \rightarrow D \rightarrow B$ becomes available.

D. Cost Function C_u

Unlike the classical diamond network that has a pre-defined linear cost function C_p and C_e assigned to each edge and route, the cost C_u in a dynamic microsimulation setting is the real-time travel time for each vehicle using the edge. When a vehicle is making the decision of which route to take, it predicts the travel time it might experience on all possible routes, and chooses the one that would result in the lowest travel time.

In a microsimulation environment, each vehicle operates with its own acceleration/deceleration controller that determines the vehicle kinematics conditioned on its surrounding traffic, for example, following the IDM model that is described in Equation 6:

$$s^*(v, \Delta v) = s_0 + \max\left[0, \left(vT + \frac{v\Delta v}{2\sqrt{ab}}\right)\right], \quad (6)$$

where the desired distance s^* is the sum of minimum spacing s_0 and the acceleration/braking distance that is determined by the current vehicle speed v , desired headway T , relative speed Δv , maximum vehicle acceleration a , and a comfortable braking deceleration b [15].

In addition, each vehicle has its own routing controller that decides which route to take based on the real-time prediction of travel times of all potential routes. This is equivalent to the situation where all vehicles are equipped with a traveler information system that could provide information on estimated travel times (e.g. Google Maps).

There are many ways to estimate the real-time travel time of a route. The method that is developed in this study is to use the position and speed of all vehicles on an edge to

estimate the travel time of each edge, then summing up the travel times of all edges along the route to get the estimated time of the route. The idea behind this method is to estimate the travel time on an edge at each time step t using only readily-available information (speed, acceleration) without solving ODEs, providing each vehicle making the routing decision an estimation of the current traffic condition on each route.

The travel time of an edge is estimated as illustrated in Fig. 3, where d_0 is the distance between the beginning of the edge and vehicle 1 (the last vehicle on the edge), d_i is the distance between vehicle i and $i+1$, and d_n is the distance between vehicle n (the front vehicle on the edge) and the stop sign.

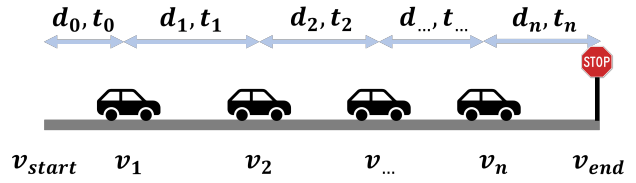


Fig. 3: Example of a stop-controlled edge with n vehicles.

Therefore, the total length of the edge should be:

$$L_{edge} = \sum_{i=0}^n d_i, \quad (7)$$

Estimated travel time of an edge:

$$C_e(edge) = \begin{cases} \frac{L_{edge}}{v_{max}} & \text{if edge is empty} \\ \sum_{i=0}^n t_i & \text{otherwise} \end{cases}, \quad (8)$$

where v_{max} is the speed limit of the edge, t_0 is the estimated time for a vehicle to travel from the beginning of the edge to the position of vehicle 1, t_i is the estimated travel time for vehicle i to travel to the position of vehicle $i+1$ and t_n is the estimated time for vehicle n to travel to the stop sign.

The decomposed travel times $t_i (i \in \{0, 1, \dots, n\})$ as labeled in Fig. 3 are calculated using a simplified estimation method. Using vehicle kinematics equations and assuming that vehicles have constant acceleration/deceleration rates, the travel time between two points (e.g. ego vehicle and a target vehicle) can be calculated as described in Algorithm 1.

The decomposed travel times t_i can then be calculated as follows:

$$t_i = \begin{cases} \text{est_tt}(v_{start}, a_i, v_1, v_{max}, a, d_i) & i = 0 \\ \text{est_tt}(v_i, a_i, v_{end}, v_{max}, a, d_i) & i = n \\ \text{est_tt}(v_i, a_i, v_{i+1}, v_{max}, a, d_i) & \text{otherwise} \end{cases}, \quad (9)$$

where v_i is the traveling speeds of vehicle i ; a_i is the acceleration of vehicle i ; v_{max} is the maximum possible speed on the edge (Equation 10); v_{start} is the assumed speed at the start of the edge, so the speed limit of the edge is used; v_{end} is the assumed speed at the end of the edge, so $1m/s$ is used since edges are controlled with stop signs; and a is

Algorithm 1 Estimate Travel Time from Current Position to Target Position (*est_tt*)

Given: speed at current position v_{ego} , current acceleration a_{ego} , speed at target position v_{target} , maximum possible speed on edge v_{max} , constant acceleration a , distance between current and target positions d

- 1: **if** a_{ego} is small **then**
 - 2: assume that vehicle travels at constant speed until it has to accelerate to reach v_{target}
 - 3: $v_{final} \leftarrow$ realized speed at target position,
 - 4: $= \min(\sqrt{v_{ego}^2 + 2ad}, v_{target})$
 - 5: $d_{accel} \leftarrow$ acceleration distance $|\frac{v_{ego}^2 - v_{final}^2}{2*a}|$
 - 6: $t_{est} \leftarrow$ time spent traveling at v_{ego} + acceleration time
 - 7: $= \frac{\max(d - d_{accel}, 0)}{v_{ego}} + \frac{2*d_{accel}}{v_{ego} + v_{final}}$
 - 8: **else**
 - 9: assume that vehicle accelerates to an intermediate speed v_i before it has to decelerates to reach v_{target}
 - 10: $v_i = \min(\sqrt{\frac{1}{2}(2*a*d + v_{ego}^2 + v_{target}^2)}, v_{max})$
 - 11: $d_{accel} = |\frac{v_{ego}^2 - v_i^2}{2*a}| + |\frac{v_i^2 - v_{target}^2}{2*a}|$
 - 12: $t_{est} = |\frac{v_{max} - v_{ego}}{a}| + |\frac{v_{max} - v_{target}}{a}| + \frac{\max(d - d_{accel}, 0)}{v_{max}}$
 - 13: **end if**
 - 14: **return** t_{est}
-

the absolute value of the assumed constant acceleration or deceleration rate (a value of $3m/s^2$ is used).

The maximum possible speed is different on turning connections than on a through connection or a straight road segment. The value of v_{max} is defined as follows:

$$v_{max} = \begin{cases} 10m/s & \text{left turn (LT)} \\ 8m/s & \text{right turn (RT)} , \\ \sqrt{2*a*length} & \text{through (TH)} \end{cases} \quad (10)$$

and note that the maximum speed on left turns and right turns is determined based on empirical observations.

Then, the cost function (travel time) of each of the 3 routes shown in Fig. 2b is

$$\begin{aligned} C_{p,A \rightarrow C \rightarrow M \rightarrow B}(t) &= C_{e,TH}(t) + C_{e,a}(t) + C_{e,TH}(t) + C_{e,b}(t) \\ &+ C_{e,RT}(t) + C_{e,b}(t) + C_{e,LT}(t) \\ C_{p,A \rightarrow N \rightarrow D \rightarrow B}(t) &= C_{e,RT}(t) + C_{e,b}(t) + C_{e,LT}(t) + C_{e,b}(t) \cdot \quad (11) \\ &+ C_{e,TH}(t) + C_{e,a}(t) + C_{e,TH}(t) \\ C_{p,A \rightarrow C \rightarrow D \rightarrow B}(t) &= C_{e,TH}(t) + C_{e,a}(t) + C_{e,RT}(t) + C_{e,c}(t) \\ &+ C_{e,LT}(t) + C_{e,a}(t) + C_{e,TH}(t) \end{aligned}$$

Based on the estimated real-time travel time of each route, each user (driver) will then select the the route that results

in the lowest cost:

$$\{C_p(t)\} = \{C_{p,A \rightarrow C \rightarrow M \rightarrow B}(t), C_{p,A \rightarrow N \rightarrow D \rightarrow B}(t), C_{p,A \rightarrow C \rightarrow D \rightarrow B}(t)\} \quad (12)$$

$$\begin{aligned} \text{selected_route}(t) &= \text{argmin}\{C_p(t)\} \\ C_u(t) &= \min\{C_p(t)\} \end{aligned} \quad (13)$$

III. EXPERIMENT SETUP

In order to numerically characterize the existence of the BP in the microsimulation environment, several parameters of the baseline and the added-path scenarios are modified to compare the performance of the networks.

First, different inflow rates of vehicles entering the network from Node 1 (Fig. 2), at 50, 200, 400, 600, 800, 900 veh/hr, are used to simulate the operations of the network with varying demand. Increasing the inflow rate would result in increased density in the system, allowing us to understand how adding a path to the network changes the ability of the system to process demands.

Second, different speed limits combinations and edge lengths are used to increase or decrease the level of attractiveness of the added path. In addition to using different lengths (50, 200, 300 and 400 meters) of all edges in the network, the speed limits of the edges other than the added path are changed from 35 m/s to 15 and 10 m/s, while fixing the speed limit of the added path ($C \rightarrow D$) to 35 m/s. The combination of edge length and speed limit determine the maximum allowable speed on the edge given a maximum acceleration. When the allowable speed on the added path is much higher than those on the other edges, the added path becomes more attractive, thus allowing us to explore how varying levels of attractiveness of the added path could impact the onset of the BP.

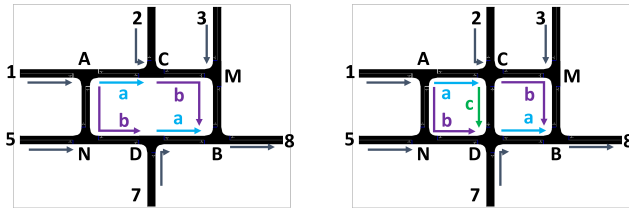
Lastly, in addition to using only one inflow node at Node 1 in Fig. 4, multiple inflow nodes (e.g. Node 2, 3, 5, and 7) are used to add additional demand to the network at once. Since each route is made of a series of edges and intersections controlled by stop signs, the flow of vehicles on each edge is dominated by the processing rate of the upstream stop sign. With multiple inflow nodes, vehicles fill up the network faster than with only one node, allowing us to compare the performance of the networks when the demand reaches near-capacity levels.

IV. RESULTS

We present how adding a path changes the overall vehicle flow, vehicle travel time and capacity of the network compared to the baseline network without any added path.

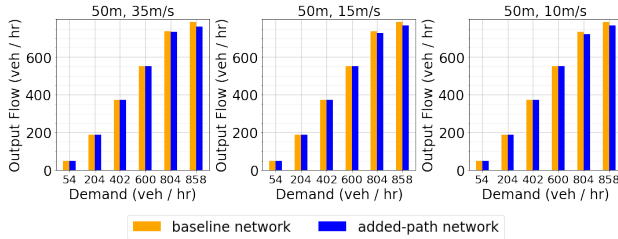
A. Impact on the Network Flow

As introduced in the experiment setup above, we explored the impact of the added path to the overall output flow of the network. Specifically, we compared how the output flow rate (measured in veh/hr) of networks, given various levels of inflow demand, differs between the baseline scenario without any additional path and the scenario with an added path.

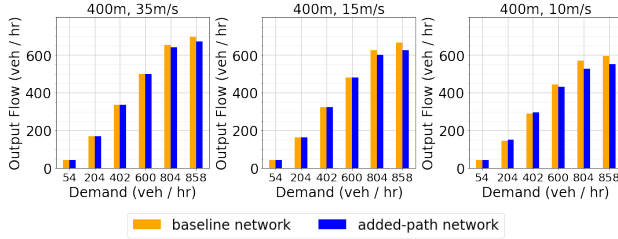


(a) Grid network with 2 routes with multiple inflow nodes (the baseline network/scenario). (b) Grid network with an added path and multiple inflow nodes (the added-path network/scenario).

Fig. 4: A 2-by-3 grid network resembling the classical diamond network with multiple inflow nodes.



(a) Output Flow vs. Demand for networks with 50-meter edges.



(b) Output Flow vs. Demand for networks with 400-meter edges.

Fig. 5: Comparison of output flow vs. demand for baseline and added-path networks.

Fig. 5 shows a comparison of the flow rates of vehicles leaving the network at different demand levels. First, we could see that when the edge length is 50 meters with speed limit variations at 35 m/s, 15 m/s, and 10 m/s (Fig. 5a), the output flow rate of the baseline scenario and the added-path scenarios are almost equal at most demand levels except for the highest one. This is because when the edge lengths are 50 meters, even though the speed limit of edges vary at different levels, the maximum achievable speed on each edge is roughly the same due to the limited distance for acceleration and deceleration. Therefore, the three plots shown in Fig. 5a are very similar. In particular, vehicle throughput is not increased despite the addition of a new road and route option.

Moreover, when the edge length is increased from 50 meters to 400 meters (Fig. 5b), the output flow of the added-path network becomes even lower than that of the baseline network as the speed limit on edges other than the added path varies from 35 m/s to 10 m/s.

Overall, the analysis of output flow rate at various demand levels in different networks shows that adding a path to the

network reduces the ability of the system to process vehicles. This reduction in output flow is more significant when the added path is more preferable and the demand level is high.

A more detailed breakdown of vehicle flow on each route in the added-path network is presented in Figure 6. When the speed limit on edges other than the added path varies from 35m/s to 10m/s while the speed limit on the added path is fixed at 35m/s, the added path becomes increasingly attractive. As shown in the stacked plot, although flow on each one of the original routes ($A-C-M-B$ and $A-N-D-B$) increases and converges to a constant as demand level increases, the flow on the shortcut route ($A-C-D-B$) increases and then decreases at an inflection point. The inflection point occurs at lower demand level as the added path becomes more attractive.

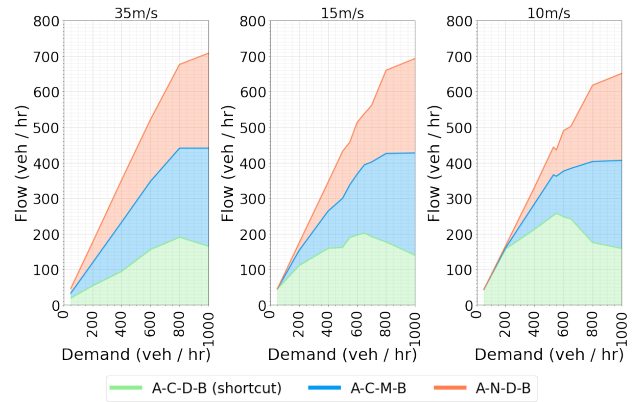


Fig. 6: Vehicle flow on each route in the added-path network with different speed limits. Each subplot shows the flow per route in added-path networks averaged over different edge length scenarios (50, 200, 300, and 400m) and the same speed limit (35m/s, 15m/s and 10m/s, respectively) on edges other than the added path, while the speed limit is fixed at 35m/s on the added path.

B. Impact on Vehicle Travel Time

In addition to comparing the output flow rate in the baseline network and the added-path one, we also compared the average travel time of vehicles in either type of the networks to determine how adding a path in the network impacts vehicle travel time.

As shown in Fig. 7, in all scenarios of different combinations of edge length and speed limits on edges other than the added path, the average travel time in the added-path network results in larger values than the baseline network when demand is large, and the added shortcut brings advantage to travel times when demand is low.

The microsimulation environment provides additional insight into the impacts of the added path on travel times. When the level of demand is low, meaning that fewer vehicles enter the system in a given time, vehicles making the routing decision will almost always choose to use the shortcut route (i.e. the route with the added path), as demonstrated in Fig. 8. These vehicles complete their trips and exit the system

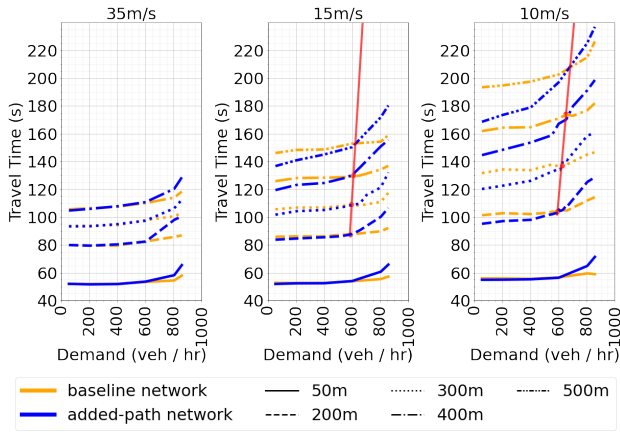


Fig. 7: Comparison of travel times at different demand level in different networks. Critical points, or the crossing points, of the lines indicate when the BP appears. An additional experiment on 500m edge length are added to test whether its critical point is the same line as the other edge length scenarios.

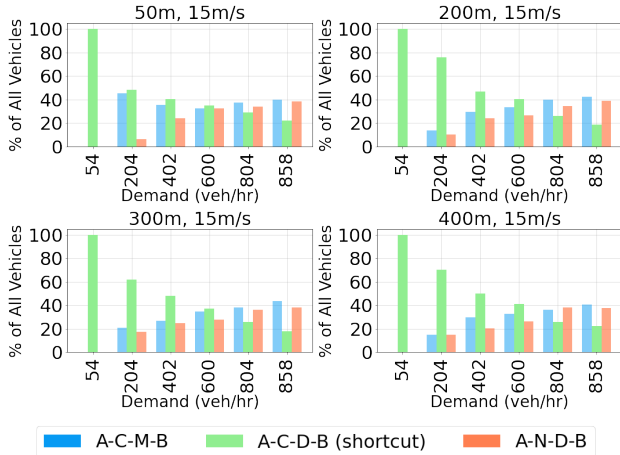


Fig. 8: Percentage of vehicles using each route with various edge lengths (50, 200, 300, and 400m) when speed limit is 15m/s on edges other than the added path while the speed limit is fixed at 35m/s on the added path.

without generating much congestion on the shortcut route, giving opportunities for future vehicles to repeat the behavior and take advantage of the shortcut route. On the other hand, when the demand level is high, vehicles enter the system at a denser rate. Since the shortcut is occupied faster and becomes less advantageous faster, the following vehicles are forced to use the other routes and the advantage of using the shortcut diminishes.

It is also worth noting that, for networks with the same speed limit on edges other than the added path, the "critical point" (i.e. where the BP shows up) appears at higher demand level as the edge length becomes longer. Critical points show strong linearity with the edge length and the demand level. As shown in Fig. 7, the fitted line from the critical points of 50, 200, 300, and 400m cases cross the critical point of the

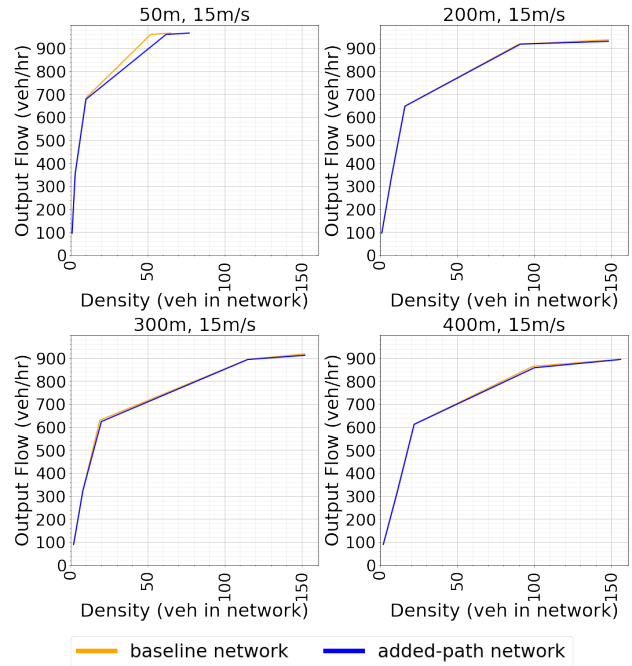


Fig. 9: Comparison of flow-density curves of both types of networks with different edge lengths and a speed limit of 15m/s on edges other than the added path.

additional 500m case.

C. Impact on Network Capacity

Although as discussed above, the results of microsimulation have shown that adding a path to the network could worsen the network performance, it is reasonable for one to wonder whether the additional physical capacity brought by the added path actually increases the operational capacity of the network. As described in experiment setup, in order to accelerate the rate at which the network approaches capacity, we added input flow to the network at Node 2, 3, 5, 7, in addition to Node 1, as labeled in Fig. 2b. We then plot the flow-density curves of the networks and compare how the capacity of the baseline and added-path networks differs.

As shown in Fig. 9, although adding a path adds more physical space to the network, the actual capacity of the added-path network is almost the same as that of the baseline network in all scenarios. This result is explained by an observation of the microsimulation runs, which reveals that even though the added path provides additional physical capacity, the attractiveness of the shortcut route results in the downstream edge of the added path (edge $D \rightarrow B$ in Fig. 2b) getting filled up faster than other edges, consequently making the shortcut route undesirable. Therefore, even though vehicles will choose to use the shortcut route at the beginning, when it is chosen by too many vehicles, the road segments upstream and downstream of the added path becomes congested, making it increasingly harder to get to the added path, thus resulting in the added path being under-utilized.

V. CONCLUSION AND DISCUSSION

In this paper, we have designed a grid network with and without an added path to explore the Braess's Paradox in the dynamic microsimulation environment. Different from existing research about BP that assigns traffic on possible routes instantaneously, we use the Flow Project and SUMO to simulate the vehicle behaviors, allowing each vehicle to dynamically choose the route with the lowest estimated travel time evaluated. By varying the edge length and speed limit, we discuss the impact of the added path on network flow, vehicle travel time, and network capacity. We find that adding a path to the network results in reduced network flow rate and vehicle flow on the added path decreases after a inflection point. In all scenarios, the added path increases the average travel times experienced by vehicles traveling through the network. Moreover, the increased congestion resulted from vehicles using the added path makes the additional physical room brought by the added path underutilized so that it does not provide more capacity to the system.

Since we discuss the BP from the microsimulation environment, we could explore how different parameters of the infrastructure affect the network performance more precisely. This is what previous dynamic traffic assignment related models can not present. A microscopic perspective provides a more advanced view on the BP, in which the impact of an added path can be characterized more finely in terms of the network characteristics. For example, while the edge costs of the static model (Fig. 1) may not be intuitively correspond to real networks, a microscopic model permits capturing realistic travel time cost functions. In the future, we would like to 1) give sensitivity analysis the design of user travel cost function; 2) explore how real-world traffic networks might suffer from the BP; 3) how traffic control strategies could bring a difference. We are also interested to more closely consider the theoretical and conceptual differences between the static and dynamic formulations.

REFERENCES

- [1] R. Steinberg and W. I. Zangwill, "The prevalence of braess' paradox," *Transportation Science*, vol. 17, no. 3, pp. 301–318, 1983.
- [2] M. Frank, "The braess paradox," *Mathematical Programming*, vol. 20, no. 1, pp. 283–302, 1981.
- [3] A. Nagurney and L. S. Nagurney, "The braess paradox," *International Encyclopedia of Transportation*. Elsevier, forthcoming. Invited chapter, pre-print available at <https://supernet.isenberg.umass.edu/articles/braess-encyc.pdf>, 2021.
- [4] S. Bittihn and A. Schadschneider, "Braess paradox in a network with stochastic dynamics and fixed strategies," *Physica A: Statistical Mechanics and its Applications*, vol. 507, pp. 133–152, 2018.
- [5] B.-B. Fu, C.-X. Zhao, and S.-b. Li, "The analysis of braess' paradox and robustness based on dynamic traffic assignment models," *Discrete Dynamics in Nature and Society*, vol. 2013, 2013.
- [6] D. E. Wolf, M. Schreckenberg, and A. Bachem, *Traffic and granular flow*. World Scientific, 1996.
- [7] R. M. Colombo, H. Holden, and F. Marcellini, "On the microscopic modeling of vehicular traffic on general networks," *SIAM Journal on Applied Mathematics*, vol. 80, no. 3, pp. 1377–1391, 2020.
- [8] A. Belov, K. Mattas, M. Makridis, M. Menendez, and B. Ciuffo, "A microsimulation based analysis of the price of anarchy in traffic routing: The enhanced braess network case," *Journal of Intelligent Transportation Systems*, pp. 1–16, 2021.

- [9] C. Wu, A. R. Kreidieh, K. Parvate, E. Vinitzky, and A. M. Bayen, "Flow: A modular learning framework for mixed autonomy traffic," *IEEE Transactions on Robotics*, 2021.
- [10] E. Vinitzky, A. Kreidieh, L. Le Flem, N. Kheterpal, K. Jang, C. Wu, F. Wu, R. Liaw, E. Liang, and A. M. Bayen, "Benchmarks for reinforcement learning in mixed-autonomy traffic," in *Conference on robot learning*. PMLR, 2018, pp. 399–409.
- [11] S. C. Dafermos and F. T. Sparrow, "The traffic assignment problem for a general network," *Journal of Research of the National Bureau of Standards B*, vol. 73, no. 2, pp. 91–118, 1969.
- [12] M. J. Smith, "The existence, uniqueness and stability of traffic equilibria," *Transportation Research Part B: Methodological*, vol. 13, no. 4, pp. 295–304, 1979.
- [13] M. Ng and S. T. Waller, "A dynamic route choice model considering uncertain capacities," *Computer-Aided Civil and Infrastructure Engineering*, vol. 27, no. 4, pp. 231–243, 2012.
- [14] Q. Meng and H. L. Khoo, "A computational model for the probit-based dynamic stochastic user optimal traffic assignment problem," *Journal of Advanced Transportation*, vol. 46, no. 1, pp. 80–94, 2012.
- [15] M. Treiber, A. Hennecke, and D. Helbing, "Congested traffic states in empirical observations and microscopic simulations," *Physical review E*, vol. 62, no. 2, p. 1805, 2000.